The Holocene temperature conundrum

Zhengyu Liu[a,b,1], Jiang Zhu[a], Yair Rosenthal[c], Xu Zhang[d], Bette L. Otto-Bliesner[e], Axel Timmermann[f], Robin S. Smith[g], Gerrit Lohmann[d], Weipeng Zheng[h], and Oliver Elison Timm[i]

[a]Nelson Center for Climatic Research and Department of Atmospheric and Oceanic Sciences, University of Wisconsin-Madison, Madison, WI 53706; [b]Laboratory of Climate, Ocean, and Atmosphere Studies, Peking University, Beijing 100871, China; [c]Institute of Marine and Coastal Sciences and Department of Earth and Planetary Sciences, Rutgers University, New Brunswick, NJ 08901-8521; [d]Alfred Wegener Institute for Polar and Marine Research, D-27570 Bremerhaven, Germany; [e]Climate and Global Dynamics Division, National Center for Atmospheric Research, Boulder, CO 80307-3000; [f]International Pacific Research Center, School of Ocean and Earth Science and Technology, University of Hawaii, HI 96822; [g]National Centre for Atmospheric Science-Climate, Department of Meteorology, University of Reading, Reading RG6 6BB, United Kingdom; [h]State Key Laboratory of Numerical Modeling for Atmospheric Sciences and Geophysical Fluid Dynamics, Institute of Atmospheric Physics, Chinese Academy of Sciences, Beijing 100029, China; and [i]Department of Atmospheric and Environmental Sciences, University at Albany, State University of New York, Albany, NY 12222

Edited by Mark A. Cane, Lamont Doherty Earth Observatory of Columbia University, Palisades, NY, and approved July 15, 2014 (received for review April 21, 2014)

A recent temperature reconstruction of global annual temperature shows Early Holocene warmth followed by a cooling trend through the Middle to Late Holocene [Marcott SA, et al., 2013, *Science* 339(6124):1198–1201]. This global cooling is puzzling because it is opposite from the expected and simulated global warming trend due to the retreating ice sheets and rising atmospheric greenhouse gases. Our critical reexamination of this contradiction between the reconstructed cooling and the simulated warming points to potentially significant biases in both the seasonality of the proxy reconstruction and the climate sensitivity of current climate models.

global temperature | Holocene temperature | model-data inconsistency

In the latest reconstruction of the global surface temperature throughout the Holocene (1) (hereafter M13), the most striking feature is a pronounced cooling trend of ∼0.5 °C following the Holocene Thermal Maximum (HTM) (∼10–6 ka) toward the late Holocene, with the Neoglacial cooling culminating in the Little Ice Age (LIA; ∼1,800 common era) (Fig. 1, blue). Numerous previous reconstructions have shown cooling trends in the Holocene, but most of these studies attribute the cooling trend to regional and/or seasonal climate changes (2–6). The distinct feature of the M13 reconstruction is that it arguably infers the cooling trend in the global mean and annual mean temperature. This inferred global annual cooling in the Holocene is puzzling: With no direct net contribution from the orbital insolation, the global annual mean radiative forcing in the Holocene should be dominated by the retreating ice sheets and rising atmospheric greenhouse gases (GHGs), with both favoring a globally averaged warming. Therefore, how can the global annual temperature exhibit a cooling trend in response to global warming forcing? This inconsistency between the reconstructed cooling and the inferred warming forced by GHGs and ice sheet poses the so-called Holocene temperature conundrum and will be the subject of this study. Here, we study the global annual temperature trend in the Holocene and its physical mechanism by comparing the temperature reconstruction with three different transient climate model simulations. Our analysis shows a robust warming trend in current climate models, opposite from the cooling in the M13 reconstruction. This model-data discrepancy suggests potentially significant biases in both the reconstructions and current climate models, and calls for a major reexamination of global climate evolution in the Holocene.

Model Experiments

We analyzed transient climate simulations in three coupled ocean–atmosphere models [Community Climate System Model 3 (CCSM3) (7), Fast Met Office/UK Universities Simulator (FAMOUS) (8), and Loch-Vecode-Ecbilt-Clio-Agism Model (LOVECLIM) (9); *Methods*] that are subject to realistic climate forcings of orbitally driven insolation variations, GHGs, continental ice sheets, and the associated meltwater fluxes. The three models all simulate a robust annual mean warming (∼0.5 °C) throughout the Holocene (Fig. 1, black and yellow), leaving a model-data inconsistency in global annual temperature of ∼1 °C. This inconsistency affects model-data comparison of the temperature trend mainly for the Holocene, rather than the last millennium (after ∼1 ka) or the early deglaciation (before ∼10 ka). In the last millennium, climate models indeed generate a global cooling toward the LIA, after the imposition of realistic volcanic aerosols and solar variability (10) (Fig. 1, *Inset*, gray line), consistent with the M13 reconstruction. During the early deglaciation and mainly in response to the large increase of atmospheric GHGs, both the data and model show a large deglacial warming (3–4 °C) that is much larger than the data-model inconsistency (11) (Fig. 1).

The forcing mechanisms of the simulated global warming are further assessed with transient sensitivity experiments that are forced by the prescribed variations in GHGs, orbital (ORB) insolation, ice sheet (ICE), and meltwater flux (MWF) individually, with other model forcings/settings fixed at the Last Glacial Maximum (∼21 ka). These forcings can be considered independent external forcings from the perspective of our coupled physical ocean–atmosphere system here, although they are all ultimately caused by the orbital forcing from the comprehensive perspective of a coupled physical-biogeochemical earth system. It should also be pointed out that no volcanic forcing and solar variability are imposed throughout the Holocene in our CCSM3 transient simulations here, a point to be returned to later. In all three models (Fig. 2 *A*–*C* and *SI Text 1*), each forcing

Significance

Marine and terrestrial proxy records suggest global cooling during the Late Holocene, following the peak warming of the Holocene Thermal Maximum (∼10 to 6 ka) until the rapid warming induced by increasing anthropogenic greenhouses gases. However, the physical mechanism responsible for this global cooling has remained elusive. Here, we show that climate models simulate a robust global annual mean warming in the Holocene, mainly in response to rising CO_2 and the retreat of ice sheets. This model-data inconsistency demands a critical reexamination of both proxy data and models.

Author contributions: Z.L. designed research; J.Z., X.Z., B.L.O.-B., and A.T. performed research; Y.R., B.L.O.-B., A.T., R.S.S., G.L., W.Z., and O.E.T. contributed new reagents/analytic tools; J.Z. analyzed data; and Z.L. wrote the paper.

The authors declare no conflict of interest.

This article is a PNAS Direct Submission.

Freely available online through the PNAS open access option.

[1]To whom correspondence should be addressed. Email: zliu3@wisc.edu.

This article contains supporting information online at www.pnas.org/lookup/suppl/doi:10.1073/pnas.1407229111/-/DCSupplemental.

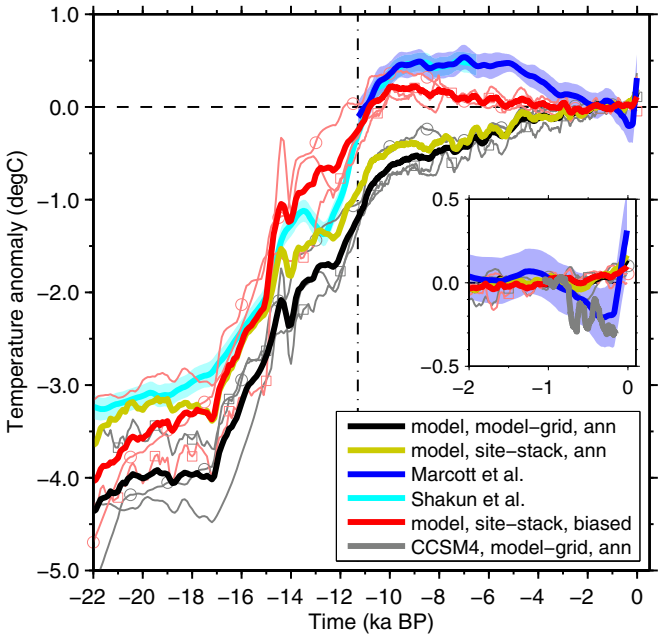

Fig. 1. Evolution of the global surface temperature of the last 22 ka: the reconstructions of M13 (1) (blue) after 11.3 ka and by Shakun et al. (11) (cyan) before 6.5 ka, the model annual mean temperature averaged over the global grid points (black), and the model seasonally biased temperature averaged over the proxy sites (red). The models are the CCSM3 (7), FAMOUS (8), and LOVECLIM (9), with the ensemble mean shown by heavy solid lines and individual members shown by light thin lines [the LOVECLIM (○) and FAMOUS (□) are marked]. Each temperature curve is aligned at 1 ka. The ensemble mean model annual temperature averaged over proxy sites is also shown (yellow, individual models for the Holocene in Fig. 3), whose similarity to the model grid average demonstrates the insensitivity of the temperature trend to the average scheme. (*Inset*) Expanded part after 2 ka, with the addition of the last millennium experiment in the CCSM4 (gray), which is forced additionally by volcanic aerosol and solar variability (10). ann, annual.

drives a weak global annual temperature response in the Holocene comparable to or weaker than the total trend (~0.5 °C), and their sum (Fig. 2 *A*–*C*, gray) largely reproduces the warming trend under the full forcing (Fig. 2 *A*–*C*, black). As expected, the warming trend in the Holocene is forced mainly by the retreating ice sheet (Fig. 2 *A*–*C*, green) and the rising GHGs (Fig. 2 *A*–*C*, orange). The discrepancy between the cooling trend in data and the warming trend in models reflects the Holocene temperature conundrum, and demands a critical reexamination of the global annual temperature trend in the Holocene in both the data and model.

Uncertainty in Temperature Reconstruction

We first examine if the cooling trend in M13 could be attributed partly to biases in the temperature reconstruction, in particular, the sea surface temperature (SST). Previous studies have suggested significant uncertainty in annual mean SST reconstructions because of the diverging trends between the alkenone-based SST and Mg/Ca-based SST (12, 13). This uncertainty is particularly problematic for the Holocene because of the small changes of annual SSTs in this period. Indeed, in the Holocene, alkenone reconstructions from the eastern tropical Pacific Ocean and South China Sea show SST warming from the Early to Late Holocene (13), whereas the Mg/Ca reconstructions from the western Pacific warm pool show a cooling trend (14). In the North Atlantic, alkenone reconstructions suggest a strong cooling trend through the Holocene, whereas Mg/Ca reconstructions show relatively stable SST or a slight warming (13). In the few available records from the Southern Hemisphere, both proxies suggest SST cooling in the Early Holocene (15, 16). These discrepancies are likely related to the different ecological (e.g., depth habitat) and seasonal (e.g., production season) biases of the proxy carriers, as well as the regional distribution of the different proxy records (12, 13, 17). Therefore, the true annual SST trends in these regions remain unclear. To test the potential impact of this seasonal bias on the cooling trend, we construct an artificial seasonally biased global temperature stack in our models. This biased stack samples the surface air temperatures from the models in annual mean and the seasons suggested by the original authors, except over the Northern Hemisphere ocean sites, where the SST takes the boreal summer season (Fig. S1 and *SI Text 2*). It is interesting that the biased stack reverses the global warming to a cooling (Fig. 1, red) and bears some resemblance to the M13 reconstruction. A further examination shows that this global cooling trend in the biased global stack is associated mainly with the summer bias in the Northern Hemisphere. Fig. 3 shows the temperature evolution in the Holocene averaged over the globe, Northern Hemisphere (30–90° N), tropics (30° S–30° N), and Southern Hemisphere (90–30° S). The global cooling trend (Fig. 3*A*) is contributed overwhelmingly by a large cooling trend (1 °C) in the Northern Hemisphere in both M13 and the biased model stack (Fig. 3*B*). Physically, in the Northern Hemisphere, the seasonal insolation changes by over ~10% throughout the Holocene and is the dominant forcing for the trend of seasonal and regional temperature; a similar strong cooling trend in summer temperature has been produced in climate models over large areas of the Northern Hemisphere (3, 5). We also tested other biased schemes in the model and found that the cooling trend in the biased stack is caused mainly by replacement of the annual SSTs by the summer SSTs in the sites of alkenone in the Northern Hemisphere (Fig. S2). From the data perspective, these alkenone-based SSTs are the proxies of the five largest cooling trends in the M13 proxy stack. The removal of these five SSTs leads to no net cooling from the Early to Late Holocene in the data, whereas the removal of about half of the cooling sites leads to virtually no cooling trend left even after the Mid-Holocene (Fig. S3). This indicates that the cooling in the entire Holocene is very sensitive to the few alkenone-based SSTs in the Northern Hemisphere, whereas the cooling after the Mid-Holocene appears to be much more robust in the data.

It should be noted, however, that the seasonally biased stack, although improving the model-data discrepancy of temperature trend in the global mean, does not improve model-data inconsistency significantly across individual sites. The spatial correlation of the temperature trends across the 73 sites of M13 stack between the data, and the ensemble model temperature for the seasonally biased stack (0.01) is not significantly different from that for the annual temperatures (−0.16) (Fig. S4, Table S1, and *SI Text 3*). These poor spatial correlations across sites reflect the much larger data-model discrepancy at individual sites as studied in previous works (18). Therefore, despite the significant differences of the SST trends in different regions and across different proxies, averaged over the globe, or simply in the Northern Hemisphere, the seasonal bias of SSTs can potentially contribute to a systematic cooling trend in the M13 reconstruction (*SI Text 1*).

In addition to the SST reconstruction discussed above, the Holocene annual cooling trend has been inferred in terrestrial proxies (Fig. S1), although there has been no systematic study on potential seasonal biases across different types of terrestrial records. The terrestrial temperature in the M13 stack shows a cooling evolution similar to the global, a significant portion of which, however, is indicated with summer biases [figure S11 and table S1 of M13 (1)]. Annual temperature inferred from borehole temperature in Greenland ice cores tends to show a cooling

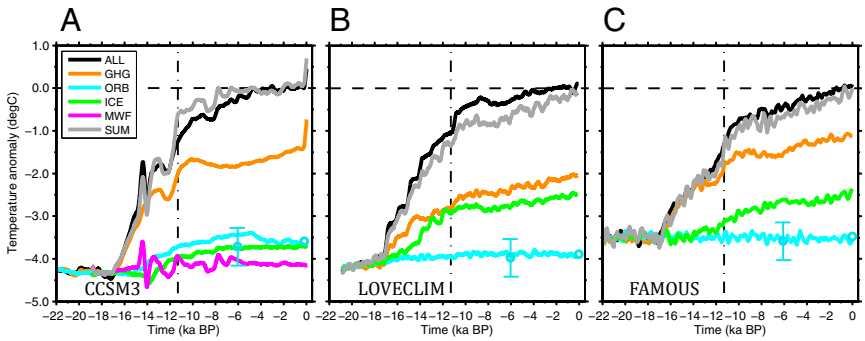

Fig. 2. Global annual mean temperature averaged over model grids under the full forcing (ALL, black) and the individual forcings [GHG, orange; orbital, cyan; ICE, green; and meltwater flux, magenta (only in CCSM3)], as well as the sum of the four single forcing simulations (SUM, gray). The PMIP temperatures are shown in ensemble means at 0 and 6 ka (cyan circles) (with 0 ka being ∼0.1 °C warmer than 6 ka) and ensemble spread (vertical bar as 1 SD). The CCSM3 (*A*), LOVECLIM (*B*), and FAMOUS (*C*) are shown.

trend (Fig. S1). A model-data comparison study suggested, however, that borehole temperatures in the Northern Hemisphere mid- and high latitudes may be biased toward warm season surface air temperature in the Early to Mid-Holocene because of the insulation effect of increased snow cover in the cold seasons (19). Ice core records in Antarctica show mixed signals, with some cooling and some warming (Fig. S1), suggesting some uncertainties in the overall temperature trend across Antarctica. The annual temperature reconstruction from an extensive dataset of terrestrial proxies in the Mid-Holocene infers an annual mean cooling from the Mid-Holocene toward the Late Holocene over much of Europe, northeastern North America, southern Africa (4), and East Asia (20), along with warming in some other regions. However, given that these reconstructions are mainly based on vegetation records, a seasonal bias and precipitation effects cannot be ruled out (2). Likewise, evidence for glacial retreats and advances in both hemispheres during the Early and Late Holocene, respectively, may also be caused by seasonal changes in precipitation and does not necessarily reflect global temperature changes (2).

Uncertainty in Climate Models

Although the potential biases in the reconstruction may contribute to the data-model discrepancy, it is also important to recognize that the data-model discrepancy can be caused by potential biases in current models. Indeed, even after considering the seasonal bias effect, the models still fail to produce some important features in the reconstruction. With the seasonally biased stack, although the model changes the annual warming to a cooling, it generates only half of the cooling in the M13 reconstruction from 10 to 1 ka (0.25 °C vs. 0.5 °C; Fig. 1 and Fig. S2). Moreover, the models simulate an almost linear cooling trend starting from the Early Holocene (∼10 ka), whereas the reconstruction exhibits the HTM (∼10–6 ka), with the cooling appearing only after the Mid-Holocene (∼5 ka).

Regardless of any climate model, it is useful to ask the following question first: What is the forcing mechanism to the coupled ocean–atmosphere system that can generate a global cooling in the Holocene? Physically, either rising GHGs or retreating ice sheets will lead to a global warming (as seen in the GHG and ICE runs in Fig. 2 *A*–*C*). Therefore, a global annual cooling, if it had occurred, can only be generated by other forcing, such as the orbital insolation and meltwater; furthermore, the cooling thus generated has to be strong enough to overwhelm the combined warming by the GHGs and ice sheets.

The orbital forcing could be a primary driver for Holocene temperature changes because it induces the largest changes of radiative flux at different latitudes and in different seasons in the Holocene (3, 5). However, averaged over the globe and the annual cycle, orbital insolation remains unchanged. Therefore, orbital forcing can alter global annual temperature only indirectly through the rectification effect of the spatially heterogeneous reflectivity and nonlinear climate feedbacks. Current climate models, however, generate a weak global annual temperature response in response to the orbital forcing (<0.5 °C), with the sign uncertain. Indeed, applying only the orbital forcing (cyan), the LOVECLIM and FAMOUS models show little change in the global annual temperature and the CCSM3 shows only a weak response: ∼0.3 °C warming from 11 to 6 ka, and a weak cooling afterward (Fig. 2 *A*–*C*). This weak orbital sensitivity is consistent with the 29 state-of-art climate models that were used in the paleoclimate model intercomparison project (PMIP) 6-ka experiments (*SI Text 4*). In these PMIP experiments, the global annual temperature shows a slight ensemble mean warming (∼0.1 °C, 18 warmings and 11 coolings), with a large ensemble spread (∼0.5 °C) (Fig. 2 *A*–*C*, cyan vertical bars). The weak model sensitivity to orbital forcing can easily be overwhelmed by the model response to GHG and ice sheet forcing. Indeed, in either GHG (Fig. 2 *A*–*C*, orange) or ICE (Fig. 2 *A*–*C*, green) experiment, the transient simulation shows a robust warming of ∼0.3 °C. This leads to a combined warming over 0.5 °C that overwhelms the weak orbital response to generate a warming of ∼0.5 °C in the full forcing simulations (Fig. 2 *A*–*C*, black).

Despite some preliminary studies (21, 22), there are so far no systematic studies on the effect of orbital forcing on global annual temperature in climate models. In principle, however, some biases could prevent a model from generating a cooling trend in the Holocene under the orbital forcing. For example, in response to the decreasing obliquity in the Holocene, a too weak, albedo-positive feedback associated with snow, ice, or vegetation at high latitudes will reduce the high-latitude cooling forced by the decreasing local annual insolation; this will bias the global temperature toward the low-latitude warming forced by the increasing annual insolation there. In response to the shift of perihelion from boreal summer to winter, the Northern Hemisphere high latitude could also bias the model toward an annual warming trend because of the reduction of the nonlinear rectification of the seasonal SST response to the decreased seasonal cycle of insolation there (23) (*SI Text 3*).

Additional feedbacks in climate models may further help in generating an annual cooling trend under orbital forcing in the Holocene. The highly uncertain cloud feedback is likely a source of model bias (24). However, given different cloud parameterization schemes across models, it is not obvious why all of the models tend to exhibit a global warming trend bias. Vegetation

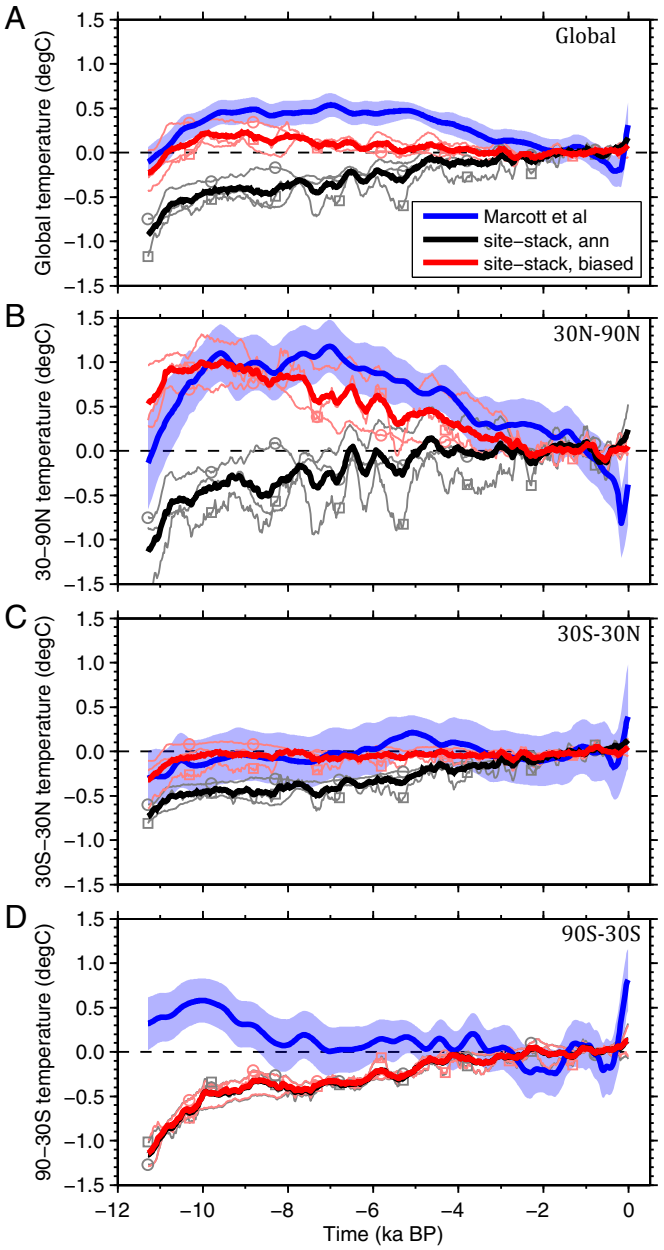

Fig. 3. Simulated global and regional mean temperatures for the last 11 ka for the three-member ensemble transient simulations and the standard 5° × 5° weighted temperature stack from the proxy dataset from M13 (blue). The models are plotted in ensemble mean (heavy solid line) and individual models (thin light lines), with the LOVECLIM (○) and FAMOUS (□) marked, for the site-stacked annual mean (black) and site-stacked seasonally biased (red). The global mean (*A*), Northern Hemisphere (30–90° N) mean (*B*), tropical (30° S–30° N) mean (*C*), and Southern Hemisphere (90–30° S) mean (*D*) are shown. The global cooling trend in the biased model global temperature stack is contributed mostly by the Northern Hemisphere bias.

feedback has been suggested to be able to induce warming in the Early to Mid-Holocene in the mid- to high-latitude boreal forest region through its impact on surface albedo (25). However, the CCSM3 and LOVECLIM both include dynamic vegetation models, which apparently are insufficient to generate a cooling trend in these models. Dust aerosol feedback, coupled with vegetation feedback, however, may provide a potential mechanism favoring a cooling trend. In the Holocene, the Afro-Asian monsoon has decreased significantly in response to the reduced summer insolation (3, 4). A weakening of the summer monsoon will lead to less vegetation cover, and therefore more dust release. The increased dust aerosol may lead to reduced insolation and, in turn, to a cooling trend in the Holocene by both the direct aerosol effect on reduced shortwaves (26, 27) and the indirect aerosol effect on increased clouds. The reduced insolation will further weaken the monsoon, forming positive feedback between the monsoon, vegetation, dust, and temperature to enhance the climate sensitivity to precession forcing in climate models. This mechanism remains to be tested in the new generation of models that include active dust and vegetation components.

It would seem to be difficult for the meltwater forcing to generate a major global mean cooling because it changes the surface temperature mainly in the interhemispheric contrast, through the heat redistribution by the Atlantic meridional overturning circulation (AMOC) (28). Even in the extreme case of a sudden shutdown of the AMOC, as in the early deglaciation (at Bølling–Allerød and Younger Dryas), global mean temperature changes only by ∼0.5–1 °C, for example, in the CCSM3 (11) (Fig. 2*A*, magenta). This modest response will be much reduced in response to a more gradual change of meltwater flux, such as that in the H1 period (19–15 ka) because of the more complete heat redistribution by the ocean–atmosphere circulation. The response will be even smaller in the Holocene because of the absence of a significant change of the AMOC in the observation (29) and the diminished meltwater flux after 6 ka.

Additional forcing, such as the volcanic forcing, may also generate a cooling trend. The cooling effect of volcanic forcing has been confirmed in current models in the last millennium, as seen in the CCSM4 simulation (Fig. 1, *Inset*). However, the volcanic forcing and solar variability are not included in our transient simulation throughout the Holocene (Fig. 2), partly because of the lack of an accurate reconstruction throughout the Holocene. The volcanic forcing can, in principle, generate a global cooling trend in current models if there is a trend of increased volcanic aerosol throughout the Holocene. However, the reconstruction of global volcanic forcing for the last 10,000 y remains highly uncertain, and there is no credible evidence of an intensification trend of volcanic activity in the Holocene (30). Even if the volcanic activity exhibited a positive trend, it would be very difficult for the volcanic forcing to generate a persistent cooling with a magnitude of over 0.5 °C from the Early Holocene to the Medieval Warm Period (MWP; ∼1 ka) as inferred in M13 (Fig. 1). This follows because the volcanic activity is already very weak at MWP, with few events and each with aerosol loading of less than ∼25 teragram (Tg) (31). Current models are able to produce a cooling of ∼0.25 °C from the MWP to the LIA, with large volcanic events of aerosols of 100–250 Tg. These models will be unable to generate a cooling of more than 0.5 °C toward the MWP, even after the elimination of the entire (weak) volcanic activity of the MWP, unless the climate sensitivity response to volcanic forcing would be 20-fold greater in the Early Holocene than in the Late Holocene.

Summarizing, neither meltwater forcing nor volcanic forcing is likely an able candidate to generate a significant global cooling trend. The biases in current models, if they exist, are more likely to be related to their sensitivity to the orbital forcing and additional feedbacks in climate models. Whatever the biases, the model biases have to exhibit a common warming bias across all of the current models with a total magnitude of at least ∼1 °C, such that removal of this model bias can generate a global cooling of ∼1 °C, which overcomes the 0.5 °C warming by GHGs and ice sheets to leave a net cooling of 0.5 °C as in the M13 reconstruction.

Conclusion

The significant discrepancy between the Holocene global cooling inferred from proxy reconstructions and simulated warming

in climate models reflects the Holocene temperature conundrum, which poses an important test for our understanding of climate changes and for the evaluation of climate models of their climate sensitivity to GHGs, ice sheets, orbital insolation, and volcanic forcings. Given the current uncertainties in both the reconstruction and model sensitivity, however, this model-data discrepancy could be attributed to either the seasonal bias in the SST reconstructions or the model bias in regional and seasonal climate sensitivity. If the M13 reconstruction is correct, it will imply major biases across the current generation of climate models. To provide a credible benchmark for future climate models, however, the proxy reconstructions will also need to be reexamined critically.

Methods

The three transient simulations of the last 21,000 y are made in three climate models: two coupled ocean–atmosphere general circulation models, the National Center for Atmospheric Research CCSM3 (7) and FAMOUS (8), and one earth system model of intermediate complexity, the LOVECLIM (9). The CCSM3 and LOVECLIM are each also coupled to a dynamic vegetation model, such that vegetation–climate feedbacks are also incorporated. Starting from before 22 ka, the models are integrated to the present subject to the realistic climate forcings of atmospheric GHG concentration, orbital insolation, the continental ice sheets, and the meltwater fluxes (but not the realistic change of volcanic aerosol and solar variability). The CCSM3 is integrated synchronously with the full forcing (32), whereas the LOVECLIM and FAMOUS are integrated without the meltwater forcing. In addition, all of the forcings in the FAMOUS are accelerated by 10-fold. The annual mean global surface temperature in each model simulation is calculated with the area-weighted average of the annual mean values on all model grids (e.g., Fig. 1, black, and Fig. 2, all curves). To compute the site-stacked surface temperature of each model, similar to M13 (1), we first interpolate the model annual mean surface temperature into the site locations using the bilinear interpolation, then take the arithmetic mean of the sites within the same 5° × 5° box, and finally do an area average of the available 5° × 5° boxes (the three-model ensemble mean is shown in yellow in Fig. 1). To compare the temperature trend in the model and observations during the Holocene directly, all of the time series are aligned at 1 ka by removing the average values between 1.5 and 0.5 ka. Because this work mostly concentrates on the temperature trend, rather than the variations at centennial and shorter time scales, all of the time series are smoothed by a 300-y moving average. Overall, the different model settings and average schemes do not have a significant impact on the global temperature evolution: All models, whether averaged over model grids or proxy sites, show a robust warming trend for annual mean global temperature (Fig. 1).

ACKNOWLEDGMENTS. We thank S. Marcott, E. Brook, and M. Mann for helpful discussions. This work is supported by National Science Foundation, Chinese National Science Foundation Grant NSFC41130105, the Department of Energy, and Chinese Ministry of Science and Technology Grant 2012CB955200.

1. Marcott SA, Shakun JD, Clark PU, Mix AC (2013) A reconstruction of regional and global temperature for the past 11,300 years. *Science* 339(6124):1198–1201.
2. Wanner H, et al. (2008) Mid- to late Holocene climate change: An overview. *Quat Sci Rev* 27:1791–1828.
3. COHMAP MEMBERS (1988) Climatic changes of the last 18,000 years: Observations and model simulations. *Science* 241(4869):1043–1052.
4. Braconnot P, et al. (2012) Evaluation of climate models using palaeoclimatic data. *Nat Clim Change* 2:417–424.
5. Renssen H, et al. (2009) The spatial and temporal complexity of the Holocene Thermal Maximum. *Nat Geosci* 2:411–414.
6. Jansen E, et al. (2007) Paleoclimate. *Climate Change 2007: The Physical Science Basis. Fourth Assessment Report IPCC*, eds Solomon S, et al. (Cambridge Univ Press, Cambridge, UK), pp 433–497.
7. Liu Z, et al. (2009) Transient simulation of last deglaciation with a new mechanism for Bolling-Allerod warming. *Science* 325(5938):310–314.
8. Smith R, Gregory J (2012) The last glacial cycle: Transient simulations with an AOGCM. *Clim Dyn* 38:1545–1559.
9. Timm O, Timmerman A (2007) Simulation of the last 21,000 years using accelerated transient boundary conditions. *J Clim* 20:4377–4401.
10. Landrum L, et al. (2013) Last millennium climate and its variability in CCSM4. *J Clim* 26: 1085–1611.
11. Shakun J, et al. (2012) Global warming preceded by increasing carbon dioxide concentrations during the last deglaciation. *Nature* 484(7392):49–54.
12. Mix A (2006) Running hot and cod in the eastern equatorial Pacific. *Quat Sci Rev* 25: 1147–1149.
13. Leduc G, Schneider R, Kim J-H, Lohmann G (2010) Holocene and Eemian sea surface temperature trends as revealed by alkenone and Mg/Ca paleothermometry. *Quat Sci Rev* 29:989–1004.
14. Linsely B, Rosenthal Y, Oppo D (2010) Holocene evolution of the Indonesian throughflow and the western Pacific warm pool. *Nat Geosci* 3:578–583.
15. Pahnke K, Sachs J (2006) Sea surface temperatures of southern midlatitudes 0-160 kyr B.P. *Paleoceanography* 21:PA2003.
16. Calvo E, Pelejero C, Deckker P, Logan G (2007) Antarctica deglacial pattern in a 30 kyr record of sea surface temperature offshore South Australia. *Geophys Res Lett* 34: L13701.
17. Mix AC, et al. (2000) Alkenones and multi-proxy strategies in Paleoceanographic studies. *Geochemistry, Geophysics, Geosystems*, 10.1029/2000GC000056.
18. Lohmann G, Pfeiffer M, Laepple T, Leduc G, Kim J-H (2013) A model-data comparison of the Holocene global surface temperature evolution. *Climate of the Past* 9: 1807–1839.
19. Mann M, Schmidt G, Miller S, LeGrande A (2009) Potential biases in inferring Holocene temperature trends from long-term borehole information. *Geophys Res Lett* 36: L05708.
20. Jiang D, Lang X, Tian Z, Wang T (2012) Considerable model-data mismatch in temperature over China during the mid-Holocene: Results of PMIP simulations. *J Clim* 25: 4135–4153.
21. Mantsis D, Clement A, Broccoli A, Erb M (2011) Climate feedbacks in response to changes in obliquity. *J Clim* 24:2830–2845.
22. Erb M, Broccoli A, Clement A (2013) The contribution of radiative feedbacks to orbitally driven climate change. *J Clim* 26:5897–5914.
23. Liu Z, Brady E, Lynch-Steiglitz J (2003) Global ocean response to orbital forcing in the Holocene. *Paleoceanography* 18:1041–1061.
24. Stephens G (2005) Cloud feedbacks in the climate system: A critical review. *J Clim* 18: 238–273.
25. Ganopolski A, Kubatzki C, Claussen M, Brovkin V, Petoukhov V (1998) The influence of vegetation-atmosphere-ocean interaction on climate during the mid-holocene. *Science* 280(5371):1916–1919.
26. Lambert F, et al. (2013) The role of mineral-dust aerosols in polar temperature amplification. *Nat Clim Change* 3:487–491.
27. Xu Y, Wang H, Liao H, Jiang D (2011) Simulation of the direct radiative effect of mineral dust aerosol on the climate at the last glacial maximum. *J Clim* 24:843–858.
28. Stocker T (1998) The seesaw effect. *Science* 282:61–62.
29. McManus JF, Francois R, Gherardi JM, Keigwin LD, Brown-Leger S (2004) Collapse and rapid resumption of Atlantic meridional circulation linked to deglacial climate changes. *Nature* 428(6985):834–837.
30. Zielinski GA, et al. (1994) Record of Volcanism since 7000 B.C. from the GISP2 Greenland Ice Core and Implications for the Volcano-Climate System. *Science* 264(5161):948–952.
31. Gao C, Robock A, Ammann C (2008) Volcanic forcing of climate over the last 1500 years: An improved ice core-based index for climate models. *J Geophys Res* 113: D23111.
32. He F (2011) Simulating transient climate evolution of the last deglaciation with CCSM3. PhD thesis (University of Wisconsin-Madison, Madison, WI).